Polymer Chain Rupture and the Fracture Behavior of Glassy Polystyrene

N. Mohammadi,[†,‡,§] A. Klein,[†,§,⊥] and L. H. Sperling*[,†,‡,§,∥]

Center for Polymer Science and Engineering, Materials Research Center, Department of Chemical Engineering, Department of Materials Science and Engineering, and Emulsion Polymer Institute, Whitaker Laboratory No. 5, Lehigh University, Bethlehem, Pennsylvania 18015

Received June 24, 1992; Revised Manuscript Received October 27, 1992

ABSTRACT: Uniform latexes of anionically polymerized polystyrene, M_n = 180 000, M_n = 250 000, and M_n = 420 000, were prepared by direct miniemulsification. The 1200-Å-diameter particles were cleaned, dried, and sintered, and the resulting films were annealed for various periods of time at 144 °C. The films were fractured with fine dental burr instrumentation at a depth of 4000 Å/pass. The number of chain ruptures and consumed energy per unit area were measured, as well as tensile strength. Plots of chain scissions and energy consumed vs 0.5 power of annealing time showed three regimes: mixed, peak, and recovery. Data in the mixed regime confirm portions of the de Gennes and Tirrell theory which predicts a 0.5 power dependence on annealing time and portions of the Wool theory. Using the Lake–Thomas theory, rubber elasticity theory, and bond dissociation energy, the contribution of the several mechanisms consuming energy were estimated on the basis of an energy balance approach. A mechanism involving the scissor-action opening of the 109° carbon–carbon bond and concomitant bond stretching of the about 300 bonds trapped between entanglements is consistent with the consumption of most of the energy in the later annealing stages and/or fast fracture processes. Tensile strength and the fracture energy per unit area of the films increase linearly with the number of chain scissions per unit fracture area in the first regime, as predicted by Peppas.

Introduction

The process of crack propagation in polymers requires the extension of chain segments which reside in the fracture plane to maximum elongation, and then the chains must either break or be pulled out from one side.[1,2] Fracture energy is consumed during the chain stretching process in two ways: (a) the energy for deforming the affected chain subsection to the fully extended conformation and (b) the energy necessary to bring all the bonds participating in that subsection to the breaking point before the chain actually breaks.[3] The viscoelastic dissipation part of the fracture energy covers the chain deformation in regions around the crack tip,[4] and the pulling or suction of chains from the fracture plane.[5,6] The relative contribution of these mechanisms in the consumption of fracture energy, however, is not well understood.

Popli and Roylance[7] performed a series of gel permeation chromatography (GPC) separations on polystyrene specimens damaged by mechanical crazing. They showed that the amount of covalent bond scission during crazing of amorphous polystyrene is detectable even though very small. Therefore, they proposed chain slippage as the major molecular mechanism but noted it may not be the only one associated with craze formation.

Fordyce et al.[8] measured the number of polymer chain scissions that occur during fracture of narrow molecular weight polystyrene samples via mechanical grinding by a dental burr at cryogenic temperatures. They found from 10^{17} to 10^{18} chain ruptures/m^2 of fracture surface by analyzing the resulting powder with electron spin resonance, dilute solution viscometry, and infrared spectroscopy.

Wool et al.[9] and Willett et al.[10] sliced high molecular weight polystyrene rods with an ultramicrotome at room temperature and concluded that around 7×10^{17} scissions/m^2 took place. With increasing temperature, a more favorable condition for chain pull out, they showed the number of broken bonds decreased.

Brown et al.[11] showed that the interface of two immiscible polymers can be strengthened by the presence of a diblock copolymer for which each of the two blocks is miscible with one of the homopolymers. They also demonstrated that crack propagation along the interface involves the breaking of all the copolymer chains at the junction point, increasing the toughness of the interface significantly.

This paper applies a custom built submicron grinding instrument, which uses a rheometer for rotating a dental burr, to the fracture of partially annealed uniform artificial latexes prepared from anionically synthesized polystyrene. This facilitates the simultaneous measure of the number of polymer chain scissions and the consumed fracture energy when a unit area of fracture surface is generated.

Theoretical Background

De Gennes in France, Wool and Tirrell in the U.S.A., and Kausch in Switzerland pioneered a theory known as crack healing or welding to understand the molecular processes that are involved in the fracture and healing of new surfaces in polymers. In this theory and concomitant experiments, the two pieces of a fractured sample are brought together with a slight pressure at a temperature above the T_g of the polymer for different time periods. Therefore, the polymer chains can cross the interface by reptation and make new entanglements. This molecular process eventually heals the fractured region. Then, partially annealed interfaces are refractured and mechanical properties correlated to annealing time and molecular weight. With the application of the reptation theory of de Gennes[12] and Edwards[13] and the development of the minor chain reptation theory by Kim and Wool,[14] the following models were proposed to rationalize the dependence of fracture properties on time and molecular weight:

(1) de Gennes[15] reported that

† Center for Polymer Science and Engineering.
‡ Materials Research Center.
§ Department of Chemical Engineering.
⊥ Emulsion Polymer Institute.
∥ Department of Materials Science and Engineering.

0024-9297/93/2226-1019$04.00/0 © 1993 American Chemical Society

$$G_{IC} \sim t^{1/2} \quad t < \tau \tag{1}$$

$$\sigma_f \sim t^{1/4} \quad t < \tau \tag{2}$$

where G_{IC}, σ_f, t, and τ are the fracture energy, fracture stress, annealing time, and relaxation time, respectively. He suggested that the number of bridges crossing a unit area of the interface was the controlling molecular property.

(2) Prager and Tirrell[16] obtained the following correlation for the case when the initial contact is between the surfaces which have many broken chain ends

$$\sigma_f \sim t^{1/8} M^{-1/8} \quad t < \tau \tag{3}$$

while they reported a stronger dependence on time and molecular weight when the initial contact is between surfaces which have been equilibrated against a gas phase:

$$\sigma_f \sim t^{1/4} M^{-3/4} \quad t < \tau \tag{4}$$

They also proposed the number of bridges per unit area spanning the original junction interface as the critical parameter.

(3) Kausch et al.[17] assumed that

$$\sigma_f \sim A/A_0 \times N/N_0 \tag{5}$$

where A is the contact area and A_0 is the total cross-sectional area of the interfacial bond. On the other hand, N and N_0 are the number of links formed across the interface at time t and the number of links at full annealing, respectively. They concluded that

$$\sigma_f \sim t^{1/4} \quad t < \tau \tag{6}$$

Applying their minor chain reptation model, Kim and Wool[14] concluded that the dependence of the fracture stress on annealing time and molecular weight can be expressed by

$$\sigma_f \sim t^{1/4} M^{-1/4} \quad t < \tau \tag{7}$$

They suggested that the average interpenetration distance of the polymer segments was the controlling molecular property.

Mikos and Peppas[18] developed a stochastic model to calculate the number of effective chain segments N_{eff} that cross the fracture plane and entangle about it, and so are able to support stresses. They found that

$$N_{eff} \sim (1 - 2M_e/M)/M_e^{1/2} \quad t \geq \tau \tag{8}$$

where N_{eff}, M, and M_e are the total number of effective crossings, the molecular weight of the polymer chains, and the molecular weight between entanglements, respectively. Invoking a chain scission criterion of all polymer segments forming effective crossings, they concluded that

$$G_{IC} \sim N_{eff} M_e \tag{9}$$

and

$$\sigma_f \sim N_{eff} \tag{10}$$

Application of the latex film formation process, healing of a polyinterface system, is another way of investigating the correlation of chain interdiffusion (via reptation) to mechanical buildup.[19-22] One of the most critical parts of the latex film formation process is the massive interdiffusion of the polymer chains across the particle interfaces and establishment of new entanglements in the neighboring particles. This phenomenon is believed to play a crucial role in strength buildup of the films made from latexes.[23] Initially, the spherical latexes contain entangled chains with some ends on or near the surface. After the cleaned latex powder is sintered, the particles have an approximately hexagonal close-packed shape. Then, depending on the annealing time, the polymer chains may diffuse to different extents into neighboring particles.

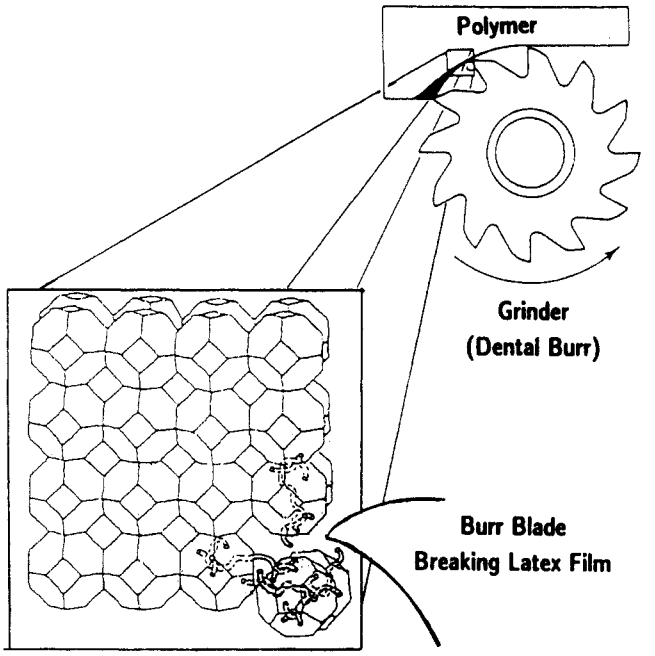

Figure 1. Schematic representation of an ideal fracture process involving the dental burr.

Table I
Direct Miniemulsification Recipes for Polystyrene Latexes[a]

ingredient	LMW	parts by weight[b] MMW	HMW
	Oil Phase		
cyclohexane	80.00	80.00	80.00
polystyrene	6.00	5.00	3.00
cetyl alcohol	1.26	1.26	1.26
stearyl alcohol	0.54	0.54	0.54
	Water Phase		
water (DDI)	200.00	200.00	200.00
sodium lauryl sulfate	2.20	2.20	2.20

[a] Sonification temperature: 50.0 °C. Sonification time: 3.0 min. [b] LMW = 220K; PDI = 1.10. MMW = 293K; PDI = 1.07. HMW = 650K; PDI = 1.08.

Before film formation is complete, the latex film can be fractured into its original particles or small clumps of them, using a suitable instrument (Figure 1). The mode of the failure of polymer chains at the interface, scission or pull out or a combination of both, will depend on the extent of polymer chain interdiffusion and establishment of new entanglements in neighboring particles. Generation of a large surface area by fracturing a polyinterface system such as the partially annealed latex films, facilitates counting of the number of chains per unit surface area that actually break during the fracture process.

Experimental Section

Direct Emulsification. Polystyrene latexes were prepared by a direct miniemulsification technique[24] based on the recipes shown in Table I. Some definitions are in order. Direct emulsification refers to submicroscopic dispersion of matter and has been practiced commercially for many years. Miniemulsification is a direct emulsification using long-chain alcohols as cosurfactants. Microemulsification uses short-chain alcohols as cosurfactants. It must be noted that the phase relations and

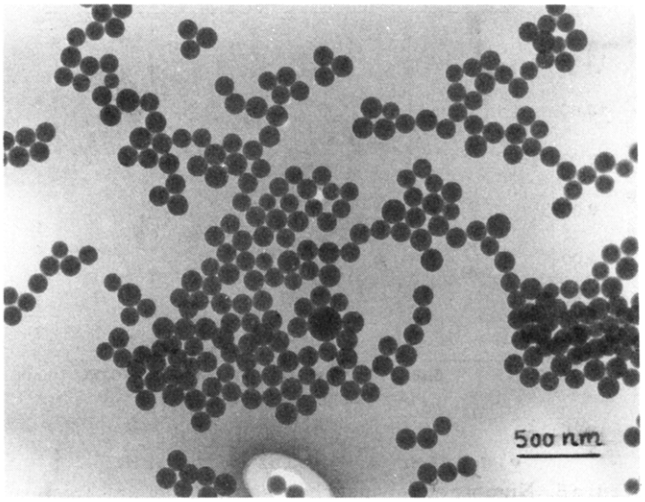

Figure 2. Transmission electron micrograph for direct miniemulsified polystyrene (M = 200 K) latex particles.

Table II
Molecular Weight and Molecular Weight Distributions of Various Polystyrenes before and after Preparation of Artificial Latexes

	molecular weights × 10^{-3}					
	original powder			in particle form		
sample	M_n	M_w	PDI	M_n	M_w	PDI
1	200	220	1.10	180	210	1.17
2	270	290	1.07	250	280	1.12
3	600	650	1.08	420	500	1.19

thermodynamics of these systems are significantly different. This paper provides an improved method of miniemulsification, such that the particles are relatively more uniform in size distribution. Since the particles also contain rather uniform molecular weight anionic polystyrenes, these materials are more suitable for polymer physics experiments.

Sodium lauryl sulfate (anionic surfactant, Fisher Scientific) was used in the water phase. Two cosurfactants, cetyl alcohol (Kodak Co.) and stearyl alcohol (Kodak Co.), were used in the oil phase. The oil phase, composed of cyclohexane, anionically synthesized polystyrene (M = 220 000, PDI = 1.1, Dow Chemical Co.; M = 290 000, PDI = 1.07, or M = 650 000, PDI = 1.08, Pressure Chemical), and two cosurfactants were mixed with the water phase, sonificated, and homogenized. The crude latexes were passed through a 0.4-μm polycarbonate (Nuclepore Inc.) membrane several times. Then, the solvent, cyclohexane, was removed by steam distillation, resulting in uniform latex particles of about 1200 Å in diameter with a polydispersity of 1.02 (Figure 2). The molecular weight distribution of these samples changed slightly after going through the particle preparation technique, but they are still less than 1.2, as summarized in Table II. The largest amount of data reported in this paper is for sample 3. The value M_n = 420 K was used in all calculations.

Characterization. Gel permeation chromatography (Waters) was applied for analyzing the molecular weights and molecular weight distributions. The clump sizes, assuming a spherical model, were measured by photon correlation spectroscopy (Coulter N4MD). Particle size and particle size distribution of the latexes were measured by transmission electron microscopy (TEM, Philips 300). A particle size dispersity index of about 1.02 was obtained on the basis of TEM (Figure 2). Differential scanning calorimetry was used to confirm the removal of surfactant and cosurfactants via glass transition measurement, a T_g of 106 °C being recorded. Scanning electron microscopy (JEOL 6300) was used to study the fracture surfaces.

Sample Preparation. The latexes were dried at 40 °C for 2 days. Then the cosurfactants, cetyl and stearyl alcohols, were removed by extraction with excess methanol for 3 days. The anionic surfactant, sodium lauryl sulfate, was removed by hot water extraction. The cleaned wet powder was dried at 40 °C. Then, the dried powder was left in 60 °C vacuum oven for 1 week to remove the possible traces of solvent. The dried polystyrene particles were sintered by using a vacuum hot press at 110 °C for 40 min under a pressure of 9.0 MPa. These conditions are just sufficient to form a void-free, fully dense film (1.05 g/cm^3), while minimizing chain interdiffusion between neighboring particles.[22]

Specimen Annealing. The resulting sintered films were about 0.8 mm thick and 37.5 mm in diameter. These were annealed at 144 °C for various periods of time in sandwich form with a steel O-ring spacer between two thin steel plates. Binder clips were used to hold the assembly together. A vacuum oven was used for annealing the samples to prevent chemical aging. Thirty minutes was allowed for temperature equilibrium, before the "annealing" times were started. After annealing, samples were quenched in a 15 °C water bath to inhibit further diffusion.

Selective Mechanical Degradation. The films were then fractured with a fine dental burr instrument[25] which cuts at a depth of 4000 Å/pass. The instrument contains three main sections: grinder, electronic module, and recorder. The grinder section has three basic parts: (a) a clock motor to rotate the head of a micrometer and a block of partially annealed sample which is glued to its spindle tip, (b) a viscometer motor which rotates the dental burr, (c) a motor that moves the viscometer motor back and forth past the sample, and a vial to collect the ground powder. A water drop at the burr tip reduces heat buildup during the grinding and collects the ground powder. The temperature increases less than 2 °C in the water drop. When the drop becomes too heavy, it falls into the vial.

Tensile Test. Tensile strength studies were carried out on partially annealed samples at room temperature by using an Instron 1011 testing machine. Dog-bone specimens (ASTM D638) were prepared by cutting the samples and grinding them with fine sand paper. A grip separation distance of 12.5 mm (gauge length) and a grip separation rate of 3 mm/min (displacement rate) were employed.

Data Analysis

Chain Scission Analysis. The number of chain scissions per unit area, N_a, was calculated using

$$N_a = \rho A \frac{d}{6}(M_n^\circ - M_n)/M_n^\circ M_n \qquad (11)$$

where A is Avogadro's number, ρ is the density, d is the average clump diameter, and M_n° and M_n are the initial and final number average molecular weights, respectively.

Fracture Energy Analysis. The energy required for stretching the polymer chain segments to the rupture point followed by scission were calculated from the Lake–Thomas theory:[3]

$$E_s = \xi^* U^* \qquad (12)$$

where ξ^* and U^* are the number of effective chain segments crossing a unit area of fracture surface and the rupture energy per effective chain segment, respectively. The number of chain ruptures per unit fracture area in each annealing point were used as ξ^* assuming every scission was preceded by an excitation of each backbone carbon–carbon bond, stretching it to maximum extension. U^* was calculated by multiplication of the dissociation energy of the carbon–carbon bond in polystyrene (70 kcal/mol) and the number of bonds between two consecutive entanglement points (about 300).

The energy necessary to uncoil the chain segments crossing a unit area of interface was calculated using the rubber elasticity theory:[26]

$$E_u = 3kT\frac{n_e \sin^2(\phi/2)}{2} \qquad (13)$$

where k, T, n_e, and ϕ are the Boltzmann constant, the temperature, the number of the constituent bonds in the segment, and the bond angle, respectively.

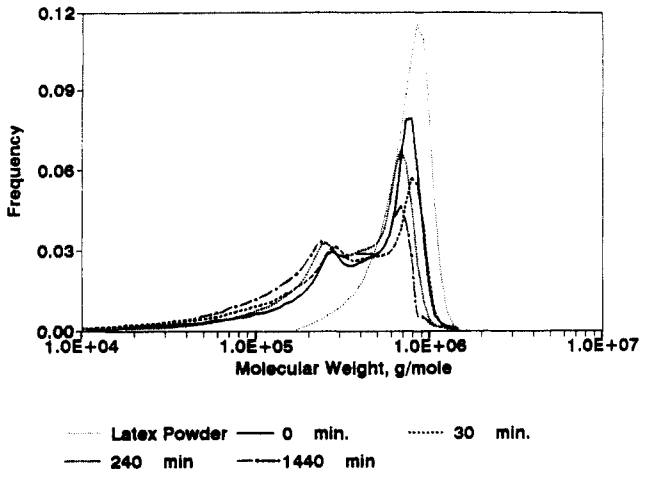

Figure 3. Gel permeation chromatograms of a ground powder of partially annealed films (M_n = 420 K), converted to read molecular weight directly.

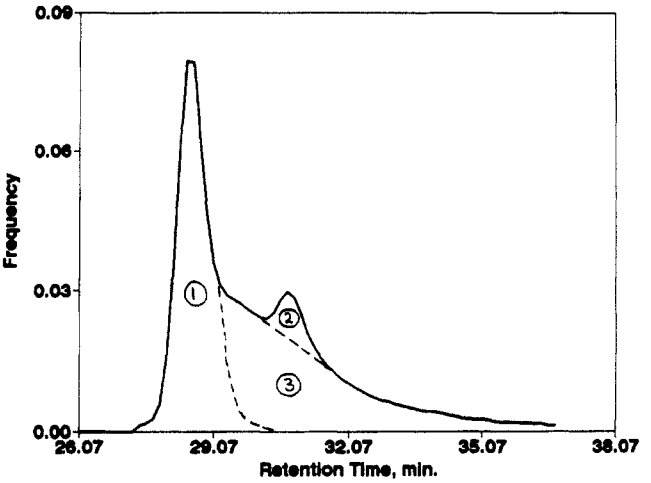

Figure 4. Schematic representation of a deconvoluted gel permeation chromatogram: (1) original peak; (2) sharp peak; (3) broad region.

Table III
Distribution of Fracture Energy among Various Micromechanisms Involved in the Fracture of M_n = 420K Artificial Polystyrene Latex Films at f = 2.65 Hz

annealing time, min	final $10^{-3}M_n$	energy consumed,[a] J/m²			
		W_U	W_S	W_V	W_T (expl)[b]
0	197	0.1	6	0	6
10	192	0.5	65	27	93
15	218	0.6	76	31	108
30	149	1.2	147	11	158
45	165	1.1	124	92	217
60	169	1.0	120	217	337
120	185	0.8	92	121	214
1440	142	1.7	197	58	255
10080	147	1.7	200	31	231

[a] W_U = uncoiling (rubber elasticity). W_S = stretch the chain segments (109° bond angle). W_V = viscoelastic processes; $W_V = W_T - (W_U + W_S)$. W_T = total energy consumed. [b] Error ±15%.

Results

Figure 3 demonstrates the molecular weight distribution of the polymer chains of a ground powder of partially annealed films for the M_n = 420 K sample. The curves were deconvoluted to three regions (original, sharp, and broad) from which their molecular weights and distributions were calculated (Figure 4). Molecular weights of ground samples are shown in Table III as a function of annealing time.

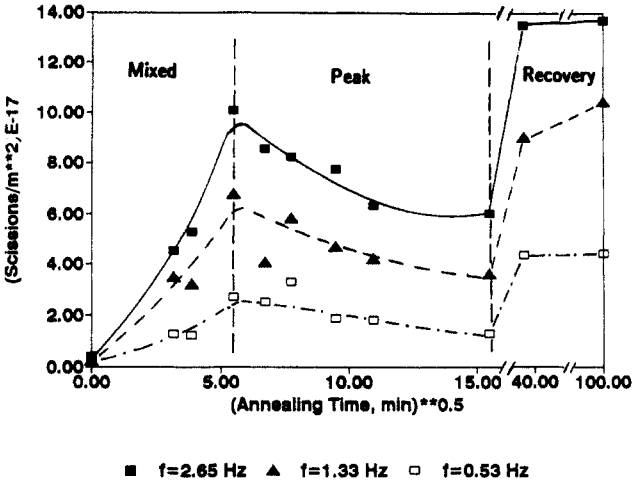

Figure 5. Number of polymer chain scissions per unit fracture surface area for M_n = 420 K at various frequencies. Note three regimes.

While the results varied slightly from sample to sample, variations were considered statistically insignificant. Typical results for the sintered sample (0 time, Table III) are shown below:

	M_n	M_w	PDI
original curve	600K	620K	1.02
sharp peak	213K	216K	1.01
broad region	127K	230K	1.81

The "broad region" might have an ideal polydispersity of 2.0 if it arises through a random cutting mechanism. The fractional contribution of each region to the overall curve varies with annealing time as follows:

annealing time, min	original curve	sharp peak	broad region
0	0.53	0.05	0.42
30	0.39	0.04	0.57
240	0.46	0.04	0.50
1440	0.29	0.05	0.65

As the annealing time increases, the original peaks diminish in size while their sharpness stays the same. The broken chains, on the other hand, increase in number and broaden the overall distribution. The sharp peak appears at around M_n = 210 K, its position and contribution changing only slightly with annealing time.

Three different mechanisms for chain breakage may cause the molecular weight distributions observed: (a) the minor chains crossing the interface of the particles[32] are broken by the growing crack; (b) multiple scission may occur as the crack advances through the threaded interface;[5,15] (c) alternatively, the propagating crack may cut the polymer chains randomly as it goes through the particles. The extent of contribution of each of these mechanisms or existence of others is not clear at this stage.

Figure 5 shows the relationship between the number of chain scissions per unit area, N_s, and the 0.5 power of annealing time for the M_n = 420 K sample at three different frequencies of burr rotation. Three regimes can be distinguished as follows:

(a) In the first regime, mixed, the chains interdiffuse sufficiently to establish new entanglements in the neighboring particles. Therefore, polymer chain rupture increases continuously as more chains cross the interface and more effective crossings form.

(b) The number of chain scissions per unit fracture area reaches a maximum around 30 min of annealing and then

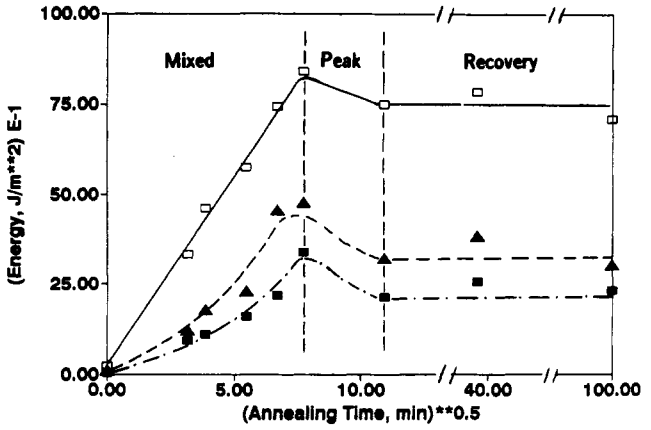

Figure 6. Fracture energy per unit area for M_n = 420 000 at various frequencies. Again, note three regines.

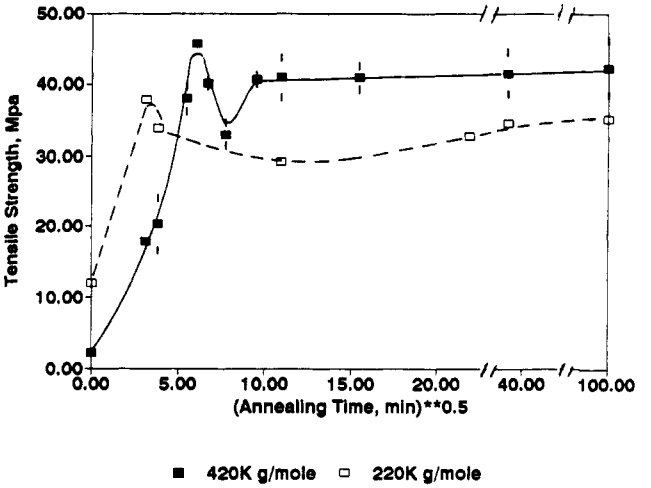

Figure 7. Tensile strength for M_n = 420 K and M_n = 200 K samples. Both samples exhibit statistically significant maxima in the tensile strength.

decreases in the peak regime. The drop may be attributed to a change in the crack growth path from the particle interface to through the particles.

(c) The polymer chains complete randomization in the recovery regime. Therefore, the number of the polymer chain ruptures per unit area recovers and continues to rise, eventually leveling off.

The reduction of the frequency of the burr rotational motion reduces the number of chain scissions per unit area. The upper and lower limits of the number of chain scissions per unit area are (a) breaking of all the chains crossing the interface (fast fracture) and (b) preferential rupturing of the effective chain crossings (slow fracture).

The number of chain scissions per unit fracture area, N_a, was found to be (1.3 ± 0.3) × 10^{18} scissions/m^2 independent of molecular weight at f = 2.65 Hz. However, they are frequency dependent as shown in Figure 5, data points on the far right. The annealing conditions were as follows:

	τ, min	t, min
M_n = 420K	96.0	10080.0
M_n = 250K	25.5	2160.0
M_n = 180K	10.5	1440.0

where t and τ are the annealing time and relaxation time of the polymer chain, respectively. The relaxation time, τ, of the M_n = 420 K sample was calculated to be 96 min at 144 °C using[27]

$$\tau = R^2/(3\pi^2 D) \qquad (14)$$

where R and D are the end to end distance of the polymer chain and the center of mass diffusion coefficient, respectively. By application of the well-known scaling equation of $D \sim M^2$, the diffusion coefficient for the M_n = 420 K sample was calculated by knowing the diffusion coefficient of M_n = 200 K.[28] Using $\tau \sim M^3$, τ values for the other two samples were calculated as shown.

Figure 6 shows the fracture energy per unit area dependence on the 0.5 power of annealing time for grinding the surface of partially annealed films of the 420 K sample at various burr rotational frequencies. Again three regimes, mixed, peak, and recovery, were observed. The fracture energy increases when the frequency decreases. The peak of the fracture energy curve occurs at around 60 min for f = 2.65 Hz while the number of scissions decrease at around 30 min of annealing. Therefore, it seems that a transition region exists in which fracture energy increases while the number of scissions decrease. With decreasing frequency, however, the transition region disappears and both curves drop at about the same time, 60 min.

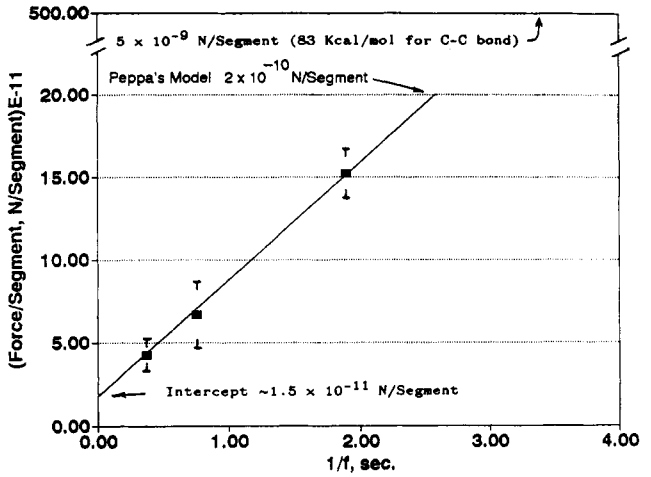

Figure 8. Force to break a segment dependent on the reciprocal of the frequency.

Figure 7 presents the tensile strength vs the 0.5 power of annealing time correlation for M_n = 420 K and M_n = 180 K samples. Again, three distinct regimes exist. The tensile strength of the lower molecular weight sample increases faster, but its overall strength is lower. The sudden dip and recovery of the tensile strength for the higher molecular weight sample is believed real, supported by triplicate testing.

Figure 8 shows the ratio of the tensile strength to the number of chain scissions per unit area as determined by the dental burr experiment, on the same sample. This is equivalent to force per chain segment and plotted as a function of frequency for the M_n = 420 K sample in the first regime. A force of about 3.5 × 10^{-11} N was calculated for breaking a segment at the highest burr frequency (2.65 Hz). With lower frequency, the force increases to 1.52 × 10^{-10} N/segment. Peppas[18] calculated a force of about 2.6 × 10^{-10} N for breaking a statistical segment based on his stochastic model.

Figure 9 demonstrates the ratio of fracture energy to the number of chain scissions per unit area plotted vs frequency. An energy as much as 2 × 10^{-16} J was calculated for stretching a segment crossing the interface to the breaking point for f = 2.65 Hz. As the frequency decreases, the energy increases to about 1 × 10^{-15} J, which is equivalent to 3.3 × 10^{-18} J/bond. A value of the order of 3.8 × 10^{-18} J/bond was calculated by Peppas.[18]

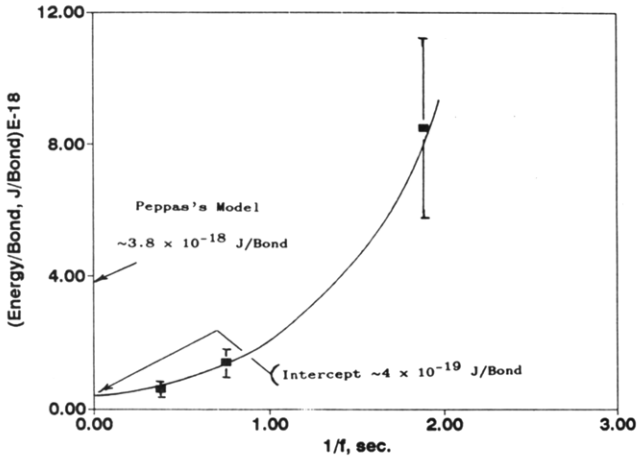

Figure 9. Fracture energy stored in a carbon–carbon bond before it breaks under external stress. The energy at infinite frequency corresponds to the actual energy of C–C bond formation.

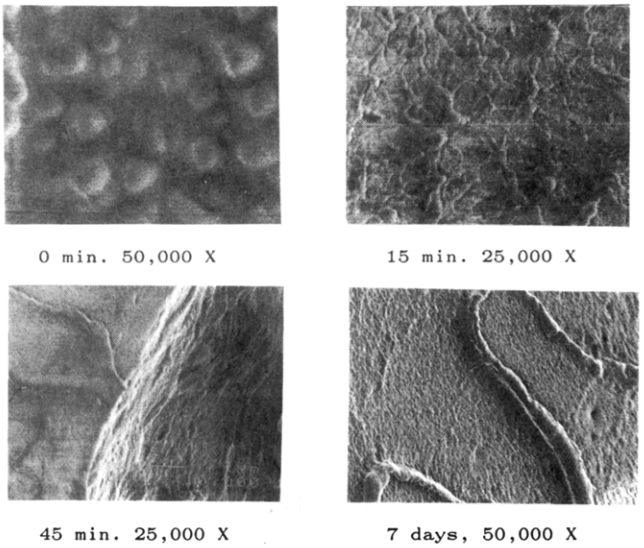

Figure 10. Scanning electron micrographs of fracture surfaces (clockwise from top left): (a) sintered film; (b) 15 min of annealing; (c) 45 min of annealing; (d) 7 days of annealing.

Most likely, this is a result of the large local shearing action of the cutter tip, during the production of shavings by the dental burr. This consumes increased shearing work in bringing the tip of the cutter to the actual state of material separation.

Figure 10 shows the surface of the partially annealed films after fracture under tension. For short annealing times (sintered sample, 0 min), M_n = 420 K, the surface appears like a basket of eggs, latex particles, when the crack goes through the particle interfaces. With an increase in the annealing time, the boundary of the latex particles begins to disappear (15-min annealing). Then (for the 45-min annealing), with an angle about 45° with respect to the original crack path, some side cracks are observed. Inside these side cracks polymer chains were fibrillated. It should be mentioned that 45 min of annealing is equivalent to the point where the tensile strength curve drops. With a further increase in annealing time (7 days), the regular fractograph of a bulk polystyrene sample appears, with patch formation and craze development.

Discussion

The fracture of films formed from emulsion-polymerized polystyrene latexes has shown four regimes.[1,2,22] Contrary to that, the first regime, an induction period, was not observed in the fracture of films prepared from artificial latexes based on anionically synthesized polystyrene (present work). Early diffusion studies by Linne' et al.[21] and Yoo et al.[22] on films prepared from emulsion polymerized polystyrene particles also showed an apparent induction period. On the other hand, Kim et al.[28] observed a fast interdiffusion from the beginning for films made from artificial latexes containing anionically prepared polystyrene. For films annealed for 1 min, M_n = 420 K, an average depth of interdiffusion of about 57 Å was calculated:[32]

$$l^2(t) = 16D^*t/\pi \tag{15}$$

where $l(t)$, D^*, and t are the average escape length of the minor chain, the segmental diffusion coefficient, and the annealing time, respectively. A segmental diffusion coefficient was calculated knowing the center of mass diffusion coefficient, annealing time, and relaxation time:

$$D/D^* = (\tau/t)^{0.5} \tag{16}$$

This depth of interdiffusion is already greater than the interdiffusion equivalent for critical entanglement molecular weight. Perhaps the first regime in the fracture properties–annealing time correlations for emulsion-polymerized films can be attributed to the induction period observed in diffusion studies. This itself may be rationalized on the basis of the ionic forces between the sulfate groups at the end of the chains which locate primarily at the surface of the particles. The interdiffusion of the polymer chains may first need a reorganization period in such a way that minimizes the interaction of the chain ends when they cross the interface. It should also be noted that at equivalent molecular weights, the anionic polystyrene diffuses about 10 times as fast as the emulsion-polymerized material.[28] This effect may be related to the size of the sulfate groups.

Reason for Peak Appearance. The drop in the fracture properties–annealing time correlations after reaching a peak was observed again. But the question is, why does this drop occur?

It may be argued that as long as the interface of the particles is healing and the crack propagates through that region, the number of chain scissions, energy consumed per unit area, and tensile strength all increase. As soon as the interface of the particles are healed sufficiently, the crack probably deviates to grow through the particles, consequently all fracture properties decrease. But the drop in tensile strength occurs in about the same time frame as the number of chain scissions does, 30 min of annealing (Figures 5 and 7). The fracture energy–annealing time curve (Figure 6), however, shows a drop at about 60 min of annealing. Therefore, a transition stage for the deflection of the crack path from the interface through the particles can be suggested.[30] In the transition zone, the crack may alternate between the interface and the chain entanglement network with possible lower entanglement density. At this stage perhaps the number of chain scissions and tensile strength decrease while more energy is consumed. The fracture surface analysis supports the idea of a transition of the crack path from the interface through the particles. The fracture surface of the sample annealed for 45 min (Figure 10), for example, when the curve just dropped in tensile strength–annealing time correlation (Figure 7) shows side cracks with an angle of about 45° to the original path. Inside these secondary cracks highly oriented fibrils were observed. The direction of fibril orientation suggests that the secondary cracks

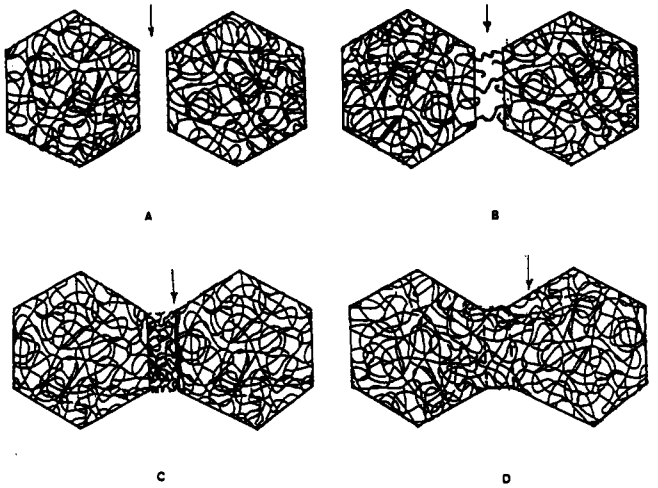

Figure 11. Schematic figure showing the interface healing process of latex films by chain interdiffusion and subsequent fracture at each stage: (A and B) crack goes through the interface of the particles, (C) crack propagates through the interface of bimodal network entanglement systems, (D) crack advances randomly.

were formed via a dual mode of two crack openings, a shear mode, which dissipates a lot of energy while reducing the chain scission phenomenon, and a tension mode. Brown observed[30] the deviation of the crack from the interface of two immiscible polymers toward the one with lower entanglement density and its jumping back to the interface, which increased the overall fracture toughness significantly.

When the crack deviates to grow through the particles, all the fracture properties decrease which may be attributed to nonequilibrium structure of the entanglement network of the chains inside the particles which may have a lower entanglement density. This entanglement network equilibrates in the long term (Figure 11D). Therefore, in the recovery regime, the number of polymer chain ruptures, fracture energy, and tensile strength all recover. The fraction of broken chains in any of these regimes is obviously controlled by the loading rate or temperature of the experiment as well as the depth of interdiffusion.

A particular model may be important here. Potter and Rudin[29] reported the property changes that result from an abrupt precipitation of polystyrene out of solutions of various concentrations. They attributed that to "trapping" of the macromolecules of these samples in a nonequilibrium entanglement condition. The same phenomena may happen when the oil-phase droplets are homogenized and the solution of polystyrene in cyclohexane is cooled to room temperature. This might result in the formation of a nonequilibrium entanglement network in the artificial latex particles (Figure 11A). Now, with annealing of the sintered films of these particles, the polymer chains interdiffuse toward the interface and form another entanglement network (Figure 11B,C). On the other hand, the network formed from entanglement of chains at the interface is created at the melt state via the reptation of the chain ends which may end in a more equilibrated network (Figure 11C).

Tensile Strength Buildup. The peak of the fracture properties–annealing time curves occurs when the chains roughly interdiffuse as far as $0.8R_g$ (~140 Å) for the M_n = 420 K sample and R_g (~130 Å) for the M_n 200 K sample which suggests a constant depth of interdiffusion equivalent of almost 2.5 bridges, $2.5M_c$, for full strength buildup. This depth of penetration, however, is a smaller fraction of the radius of gyration for higher molecular weights.

The ratio of the tensile strength of the lowest point following the peak to the highest point in the peak regime is around 0.72, while the same ratio in the fracture energy–annealing time curve is about 0.3. This difference can be argued on the basis of the different loading rates of the experiments; the tensile experiment was performed at a much slower rate. The ratio increases as the frequency of the grinding process is reduced (Figure 5). This suggests that the bimodal entanglement network supposition at the interface and the core of the particles is more detectable at higher fracture rates.

Energy Balance. Interestingly, the contribution of the chain straightening free energy, calculated through rubber elasticity,[26] turns out to be of the order 0.5 J/m^2 (Table III), 2 orders of magnitude smaller than the energy necessary to stretch the bonds (see eq 13). The important term for the fast fracture case and especially for long annealing times, is the energy well quantum mechanics contribution to stretching each carbon–carbon bond to the breaking point, W_s (Table III). The pull-out energy is thought to decrease with annealing time, because entangled chains break rather than pull out of their respective surfaces. The contribution of pull-out energy increases by reducing the fracture rate or increasing the temperature.

Using the measured temperature rise of about 1-2 deg in the drop of water during the grinding process, an energy dissipation of about 160–320 J/m^2 was calculated. An energy of about 200–400 J/m^2 was measured on the basis of torque conversion. The interesting point here is that, to a first approximation, all of the work, mechanical and chemical, is accounted for, as being eventually to heat.

Using a computer simulation approach, Cook[31] studied polymer deformation. He showed that as the interaction between the chain atoms and the surrounding medium increases, the rotational angle motion is suppressed, and large amounts of energy are stored in backbone bond angle and bond length distortion. He also argued that the homogeneity of distribution of stored energy in different bonds increases when the interaction with medium increases.

Controlling Molecular Phenomena. As the annealing time increases, two parameters, the number of chain segments crossing a unit area of the interface, $n(t)$, and the average contour length of diffused polymer chain segments across the interface, $l(t)$, increases. Consequently, the probability of establishing entanglements in the neighboring particles increases. Polymer chain segments with two entanglements in the neighboring particles are thought to be more prone to rupture during the fracture process. Therefore, the controlling molecular properties for observation should contain $n(t)$ and $l(t)$.

Wool[32] derived the time and molecular weight dependence of the total interpenetration contour length, $L(t)$, of polymer chain segments crossing a unit area of the interface for short annealing times:

$$L(t) \sim n(t)\, l(t) \sim t^{3/4}M^{-7/4} \tag{17}$$

For long annealed samples he showed

$$L(\infty) \sim M^{1/2} \tag{18}$$

Similarly, deGennes[15] and Prager and Tirrell[16] derived the scaling law for the number of bridges that cross the unit area of the interface:

$$P(t) \sim n(t)\, l(t)^{1/2} \sim t^{1/2}M^{-3/2} \tag{19}$$

For the samples well annealed above their relaxation time

$$P(\infty) \sim M^0 \quad (20)$$

The slopes of the mixed regions for Figures 5 and 6 were determined from log–log plots. There are

frequency, Hz	scissions–time	energy–time
2.65	0.76	0.67
1.33	0.65	0.77
0.53	0.72	0.51

According to deGennes and Tirrell, the slopes should be 0.50, and according to Wool, the slopes should be 0.75. While most of the data seem to favor Wool's interpretation, it must be noted that the slopes are only accurate to ±0.1. Additionally, it must be noted that the molecular weight dependence was found to be zero, supporting the theory of deGennes and Tirrell, rather than Wool.

Thus, both theories are supported in part, but with data at hand, neither seems decisively better than the other.

Conclusions

Three regimes, mixed, peak, and recovery, were found in the number of chain scissions per unit area, the total fracture energy per unit area, and the tensile strength–annealing time correlation. Variously, 0.50–0.75 power scaling relationships were found for the number of chain scissions and the fracture energy per unit area as a function of annealing time for the mixed regime, which is in between the 0.5 power dependence on time derived by deGennes[15] and Prager and Tirrell[16] and the 0.75 power dependence derived by Wool.[32] The fracture energy per unit area and tensile strength increase linearly with the number of chain scissions per unit area in the mixed regime, which agrees with the results of Peppas's[18] stochastic model for a brittle material.

Acknowledgment. The authors wish to thank the National Science Foundation for support through Grant No. CBT-8820705. We wish to thank Dr. Brian Dalke of Dow Chemical Co. for his contribution of anionically synthesized polystyrenes.

References and Notes

(1) Mohammadi, N.; Klein, A.; Sperling, L. H. *Polym. Mater. Sci. Eng.* **1992**, *66*, 416.
(2) Mohammadi, N.; Yoo, J. N.; Klein, A.; Sperling, L. H. *J. Polym. Sci., Polym. Phys. Ed.* **1992**, *30*, 311.
(3) Lake, G. J.; Thomas, A. G. *Proc. R. Soc. London, A* **1967**, *300*, 108.
(4) deGennes, P. G. *C. R. Seances Acad. Sci., Ser. II* **1988**, *307*, 1949.
(5) Mazich, K. A.; Samus, M. A.; Smith, C. A.; Rossi, G. *Macromolecules* **1991**, *24*, 2766.
(6) deGennes, P. G. *J. Phys. Fr.* **1989**, *50*, 2551.
(7) Popli, R.; Roylance, D. *Polym. Eng. Sci.* **1982**, *22*, 1046.
(8) Fordyce, P.; Fanconi, B. M.; Devries, K. L. *Polym. Eng. Sci.* **1984**, *24*, 421.
(9) Wool, R. P.; Rockhill, A. T. *J. Macromol. Sci.—Phys.* **1981**, *B20*, 85.
(10) Willett, J. L.; O'Conner, K. M.; Wool, R. P. *J. Polym. Sci., Polym. Phys. Ed.* **1986**, *24*, 2583.
(11) Brown, H. R.; Deline, V. R.; Green, P. F. *Nature* **1989**, 341.
(12) deGennes, P. G. *J. Chem. Phys.* **1971**, *55*, 572.
(13) Edwards, S. F. *Proc. Phys. Soc., London* **1967**, *92*, 9.
(14) Kim, Y. H.; Wool, R. P. *Macromolecules* **1983**, *16*, 1115.
(15) deGennes, P. G. *C. R. Seances Acad. Sci.* **1980**, *B291*, 219.
(16) Prager, S.; Tirrell, M. *J. Chem. Phys.* **1981**, *75*, 5194.
(17) Jud, K.; Kausch, H. H.; Williams, J. G. *J. Mater. Sci.* **1981**, *16*, 204.
(18) Mikos, A. G.; Peppas, N. A. *J. Chem. Phys.* **1988**, *88*, 1337.
(19) Voyutskii, S. S. *Autohesion and Adhesion of High Polymers*; Interscience: New York, 1963.
(20) Sperling, L. H.; Klein, A.; Yoo, J. N.; Kim, K. D.; Mohammadi, N. *Polym. Adv. Technol.* **1990**, *1*, 263.
(21) Linne', M. A.; Klein, A.; Miller, G. A.; Sperling, L. H. *J. Macromol. Sci.—Phys.* **1988**, *B27* (2 & 3), 217.
(22) Yoo, J. N.; Sperling, L. H.; Glinka, C. J.; Klein, A. *Macromolecules* **1990**, *23*, 3962.
(23) Mohammadi, N.; Klein, A.; Sperling, L. H. *Ukr. Polym. J.* **1992**, *1*, 22.
(24) Mohammadi, N.; Kim, K. D.; Sperling, L. H.; Klein, A. *J. Colloid Interface Sci.*, accepted.
(25) Mohammadi, N.; Bagheri, R.; Miller, G. A.; Klein, A.; Sperling, L. H. *Polym. Testing*, accepted.
(26) Prentice, P. *Polymer* **1983**, *24*, 344.
(27) Whitlow, S. J.; Wool, R. P. *Macromolecules* **1991**, *24*, 5926.
(28) Kim, K. D.; Sperling, L. H.; Klein, A. *Macromolecules*, submitted for publication.
(29) Potter, D. K.; Rudin, A. *Macromolecules* **1991**, *24*, 213.
(30) Brown, H. R. *J. Mater. Sci.* **1990**, *25*, 2791.
(31) Cook, R. *J. Polym. Sci. Polym. Phys. Ed.* **1988**, *26*, 1349.
(32) Wool, R. P.; Yuan, B. L.; McGarel, O. *J. Polym. Eng. Sci.* **1989**, *29*, 1340.